Voltage-current behavior of a superconducting STAR® wire in a 6-around-1 cable configuration

Atik Chavda, Paolo Ferracin, Hugh Higley, Nghia Mai, Goran Majkic, Prakash Parthiban, Jithin Peram, Soren Prestemon, Umesh Sambangi, Jithin sai Sandra, Kala Selvamanickam, Venkat Selvamanickam, Xiaorong Wang

***Abstract*—A 6-around-1 transposed cable using superconducting STAR® wires can be useful for future circular collider applications. We made three cable samples using single STAR® wires with a diameter of 1.3 mm. The first two samples, made with a cabling machine, used STAR® wires consisting of a 0.7 mm diameter Nb-Ti core. The third cable sample was manually wound and used a STAR® wire made with a 0.81 mm diameter Cu core. The first sample showed severe degradation after the cable was bent to a 75 mm radius. The current-carrying capability of the innermost and outermost REBCO tapes in the STAR® wire degraded by 42% to 98% and the middle REBCO tapes remained intact. This was also the case for the second and straight cable sample. After fabrication of the third cable sample, we observed only about 5% reduction in the current along the wire, measured at different locations inside the terminations. The results suggest that the differences in architecture or fabrication of the STAR® wires could have caused differences in critical current retention after cabling.**

***Index Terms*—REBCO, STAR® wire, 6-around-1 cable**

I. Introduction

THE U.S. Magnet Development Program, in collaboration with industry, is evaluating magnet conductors based on REBCO tapes for high-field accelerator magnet applications [1]. The program has been focused on two round wires, CORC® and STAR®, both commercially available [2]–[7]. Several small dipole magnets have been made and tested to provide feedback on the wire performance [8]–[10].

The diameter of a STAR® wire can be 2 mm or smaller. A bundle of such small-diameter STAR® wires can form a high-current conductor to reduce the inductance of high-field magnets. As a first step toward this goal, we recently reported a 6-around-1 cable using 1.8 mm diameter STAR® wires [11].

Although these 6-around-1 STAR® cable samples showed encouraging transport and bending performance, several questions remain open. For instance, what is the impact of cabling process on the critical current of STAR® wires? Which tapes degrade and affect the critical current of the cable? In addition, we need small-diameter STAR® wires carrying high current to increase the whole-conductor current density of a 6-around-1 cable.

To address these needs, we made three 6-around-1 cable samples. Each sample had a single 1.3 mm diameter STAR® wire developed by AMPeers. The results from this work can provide insight into understanding the voltage-current behavior of a STAR® wire. They can also help lead to a more robust fabrication process of the STAR® wires and 6-around-1 cables for high-field magnet applications [12].

II. STAR® Wires and Cable Samples

AMPeers manufactured three STAR® wires for the experiments reported here. Each wire has four REBCO tapes, one tape per layer around a core. Wires 1 and 2 used a Nb-Ti wire as the core and used tapes of three different widths. The Nb-Ti core has a higher tensile strength than that of a Cu wire of the same diameter. Wire 3 used a solid Cu wire as the core and used tapes of the same width. Table I gives the main geometric parameters for each wire.

TABLE I
Main Parameters for the Three STAR® Wires.

Parameters	Unit	Wires 1, 2	Wire 3
Innermost Tape 1 width	mm	1.5	2.0
Tape 2 width	mm	1.8	2.0
Tape 3 width	mm	1.8	2.0
Outermost Tape 4 width	mm	2.3	2.0
Core material	-	Nb-Ti	Cu
Core diameter	mm	0.70	0.81
Wire diameter	mm	1.3	
Wire length	m	1.0	1.6

We made three 6-around-1 cables, each containing a single STAR® wire, five companion Cu strands and one Cu central core. Cable sample 1e used insulated Cu strands and core throughout the entire cable, including inside the terminations at both ends of the cable. Table II lists the main parameters for the three cable samples.

Cable Samples 1e and 1f were made using a cabling machine at LBNL. We installed a flute-type electrical termination to all three cable samples. Reference [11] has more details on the cabling process and electrical termination.

Cable Sample 1h was cabled by hand to enable a direct comparison of the voltage-current behavior before and after the

Manuscript received September 16, 2024. This work was supported by SBIR award DE-SC0021689 from the U.S. Department of Energy, Office of High-Energy Physics. The work at LBNL was also supported by the U.S. Magnet Development Program through Director, Office of Science, Office of High Energy Physics of the US Department of Energy under Contract No. DEAC02-05CH11231.

A. Chavda, G. Majkic, P. Parthiban, J. Peram and V. Selvamanickam are with University of Houston, Houston, TX 77024, United States. (e-mail: selva@uh.edu).

P. Ferracin, H. Higley, S. Prestemon and X. Wang are with Lawrence Berkeley National Laboratory, Berkeley, CA 94720, United States. (e-mail: xrwang@lbl.gov).

U. Sambangi, J. Sandra, N. Mai and K. Selvamanickam are with AMPeers LLC, Houston, TX 77059, United States.

TABLE II
MAIN PARAMETERS FOR THE THREE 6-AROUND-1 CABLE SAMPLES.

Parameters	Unit	1e	1f	1h
STAR® wire from Table I	-	1	2	3
Diameter of Cu strands	mm	1.29	1.29	1.29
Diameter of Cu core	mm	1.63	1.63	1.29
Cu insulated?	-	yes	no	no
Nominal cable twist pitch	mm	53	53	53
Nominal cable diameter	mm	4.6	4.6	4.3
Cable length	m	0.98	0.98	1.57

cabling process. We first made a 6-around-1 cable using seven Cu strands, each having a diameter of 1.29 mm. The Cu cable template has the same pitch length as cable Samples 1e and 1f. We removed one of the outer Cu strands to accommodate the STAR® Wire 3. When bending Wire 3 into the 6-around-1 cable template, we tried to maintain a constant tension and to minimize the torsion on the wire. Fig. 1 shows the STAR® wire was wound into the 6-around-1 cable template.

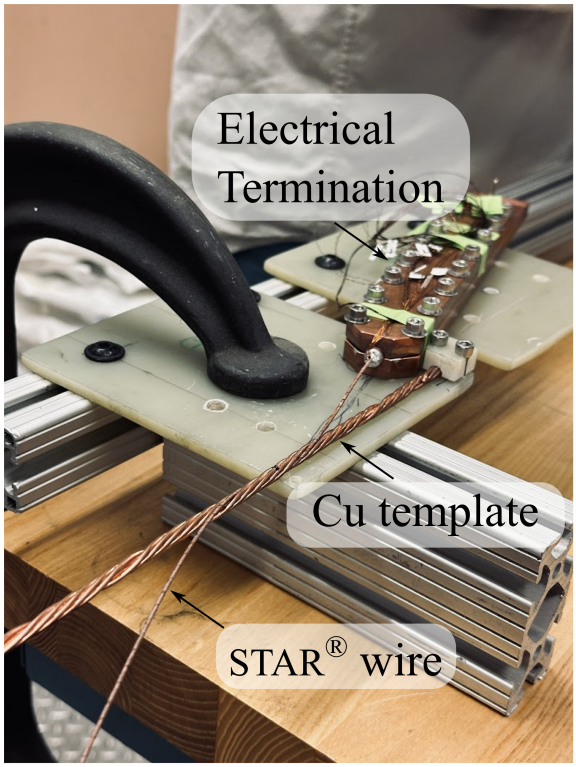

Fig. 1. A close up view of winding STAR® Wire 3 into a 6-around-1 cable template.

III. INSTRUMENTATION AND MEASUREMENT PROTOCOL

We installed three sets of voltage taps inside the electrical terminations for cable Samples 1e and 1f, following the convention as shown in Fig. 6 in [11]. The innermost taps, V_1, were inserted inside the termination before we filled the termination with molten indium. Therefore, the V_1 taps were not intentionally soldered to any specific REBCO tapes inside the terminations.

To understand the current-carrying capability of each individual REBCO tape, we added voltage taps to the outermost tapes in cable Samples 1e and 1f and measured the voltage as a function of current. We soldered the voltage taps, using Sn60Pb40, on the tape between the terminations. The voltage taps were about 50 mm away from the termination. We started from Tape 4, the outermost tape (Fig. 2). After Tape 4 was measured, we warmed up the cable sample and cut Tape 4 at both ends so the tape was isolated from the terminations. After Tape 4 was isolated, we exposed Tape 3 and soldered a pair of taps to it. The cable was cooled down and tested again at 77 K. We repeated the process until we measured the voltage across Tape 1, the innermost tape of cable Samples 1e and 1f.

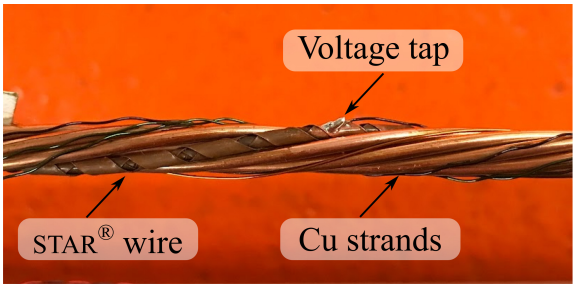

Fig. 2. A voltage tap was soldered to Tape 4, the outermost tape of the STAR® wire in cable Sample 1f. The nearest flute-type termination, not shown here, was about 5 cm to the left of the voltage tap.

For Wire 3, we soldered a voltage tap to each tape inside the terminations. To ensure that the tap remained connected on the tape when installing the termination, we wrapped a solid fine Cu wire around the tape for three turns (Fig. 3). Then we soldered the Cu wire to the tape using indium and trimmed the tape to expose the tape beneath. These voltage taps were in addition to the V_1 tap.

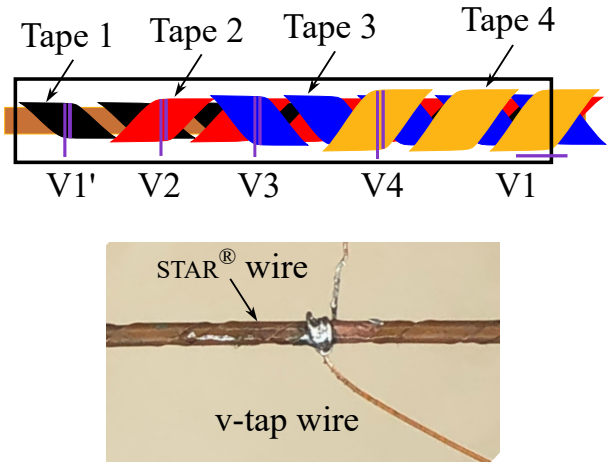

Fig. 3. Top: a schematic showing a voltage tap is attached to each of the four tapes inside the termination of Wire 3. Black box: flute-type termination. Purple lines: solid Cu instrumentation wires. V_1 tap is not intentionally attached to any tape. Bottom: a picture showing a voltage-tap wire wrapped and soldered around a tape before trimming the tape.

We measured the $V(I)$ behavior of Sample 1e at different bend radii. At each radius, we bent the sample around a printed circular former for at least 180° to cover multiple pitch lengths along the cable sample. More details can be found in [11].

Samples 1f and 1h were only measured straight without bending.

All three samples were tested in liquid nitrogen at 77 K, self-field. We increased the current in a stair-step fashion. The voltages were measured by Keithley 2182A nanovoltmeters when the current was held constant. The current was measured by a resistive shunt with an uncertainty of ± 0.5 A.

IV. Results

A. Cable Sample 1e, bent to 20 mm radius

Fig. 4 shows the V_1 voltage across the cable in different bending radii. We also included the voltage across the wire measured at AMPeers before cabling.

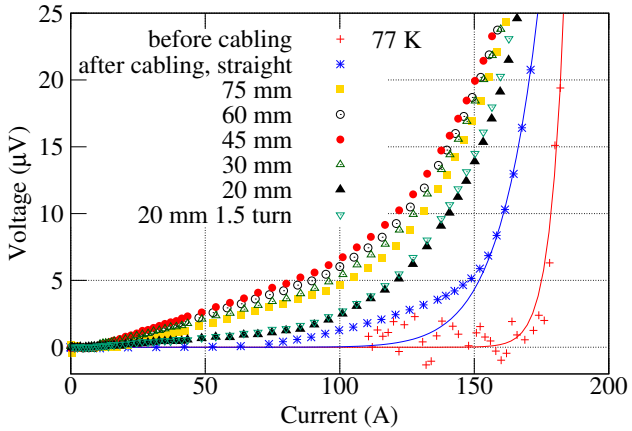

Fig. 4. The voltage measured from the V_1 taps across cable Sample 1e at different bending radii. The voltage across the wire measured at AMPeers before cabling was also included. The red and blue lines are the power-law fit according to (1). 77 K, self-field.

We used a power law to characterize the measured $V(I)$ data,

$$V = V_{\text{offset}} + IR + V_c \left(\frac{I}{I_c}\right)^n, \qquad (1)$$

where V_{offset} is the voltage offset, R is the termination resistance, and V_c is the voltage criterion. We used 20 μV as the voltage criterion for the I_c reported here.

Fig. 5 shows the voltage on each outermost tape after removing the previous outermost tape, in addition to the V_1 voltage.

We defined the reduction in the critical current, as determined from the $V_1(I)$ data, as the critical current of the tape that was removed. Table III gives the critical current of each tape measured with cable Sample 1e at a 20 mm bend radius. The critical current of Tapes 1 and 4 significantly degraded compared to the critical current measured by AMPeers on 10 cm long witness tapes similar to the tapes that were made into the STAR® wire.

B. Cable Sample 1f, straight without bending

Cable sample 1f showed an early voltage rise before bending, similar to cable Sample 1e (Fig. 6). We decided to measure the voltage across each tape without bending the cable. Fig. 6 shows the V_1 voltage as a function of current and the voltage on each outermost tape after removing the previous one.

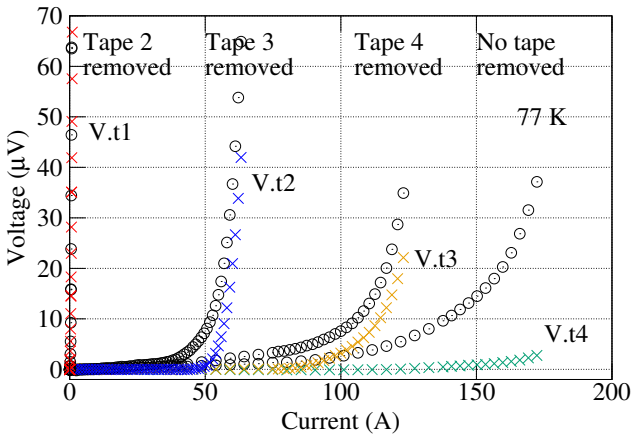

Fig. 5. The voltage measured from the V_1 taps and the voltage taps on the current outermost tape after the previous one was isolated from the terminations in cable Sample 1e. Open circles: V_1. Crosses: voltage on a single tape. The resistive voltage due to joint resistance is removed. 77 K, self-field.

TABLE III
Comparison between the critical current measured on cable Sample 1e at 20 mm bend radius and on witness tapes at AMPeers. 77 K, self-field.

Tape	AMPeers (A)	LBL (A)	ΔI_c (-)
4	72	42	−42%
3	51	59	13%
2	51	57	12%
1	43	1	−98%

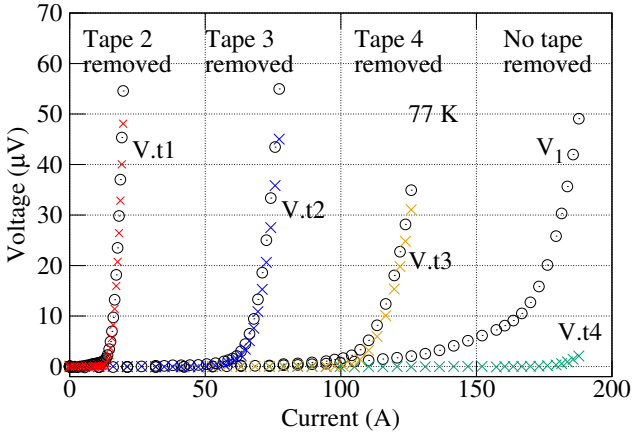

Fig. 6. The voltage measured from the V_1 taps and the voltage taps on the current outermost tape after the previous one was isolated from the terminations in cable Sample 1f. Open circles: V_1. Crosses: voltage on a single tape. The resistive voltage due to the joint resistance was removed. 77 K, self-field.

Table IV compares the critical current of each tape in cable Sample 1f to the critical current measured by AMPeers on the witness tapes similar to the tapes that were used in the STAR® wire. Tapes 1 and 4 degraded most among the four tapes.

As we removed the outermost tapes, the resistive slope of the measured $V_1(I)$ data, partially due to the termination resistance, increased. It was 49 nΩ when all four tapes were

TABLE IV
COMPARISON BETWEEN THE CRITICAL CURRENT MEASURED ON CABLE SAMPLE 1F AND ON WITNESS TAPES AT AMPEERS. 77 K, SELF-FIELD.

Tape	AMPeers (A)	LBL (A)	ΔI_c (-)
4	75	51	-32%
3	51	50	-2%
2	51	53	4%
1	44	17	-59%

connected. The resistance increased to 268 nΩ when only the innermost tape was connected.

With only the innermost tape remaining in the STAR® wire, we measured the $V(I)$ behavior of the cable at different bend radii at 75, 60, 45, 30 and 20 mm. At every radius, the sample was bent for 180°.

The critical current of cable Sample 1f with only the innermost tape was 17.4 A before bending, decreased from 17.0 A at a 20 mm bend radius. The n value increased from 8.3 before bending to 8.6 based on the power-law fitting.

C. Cable Sample 1h, manually cabled

Fig. 7 shows the voltage as a function of current measured from the taps soldered on each tape inside the terminations, before and after the manual cabling process.

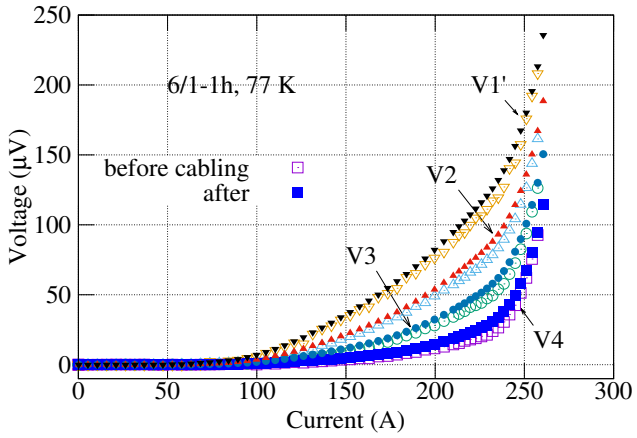

Fig. 7. The voltage measured from the taps soldered on each tape inside the terminations before and after cabling. Open symbols: before cabling. Closed symbols: after cabling. The resistive voltage due to joint resistance was removed. 77 K, self-field.

Table V gives the current, n value and resistive slope determined from each voltage signal according to (1) using a voltage criterion of 20 μV. We fit to a peak voltage of about 25 μV. The n values ranged from 6 to 12 when fitting the $V(I)$ data for the current above 240 A.

V. DISCUSSION

The $V(I)$ curve of cable Sample 1e indicated significant degradation in the critical current after we bent the cable from straight to a radius of 75 mm (Fig. 4). The overall voltage across the cable sample reduced when the cable was bent to 20 mm, likely due to better electrical contact between the tapes in the STAR® wire under compression. The onset current when the voltage started rising, around 10 A, remained the same as larger bend radii.

The innermost and outermost tapes in the STAR® wire in cable Sample 1e degraded most and the critical current of the middle two tapes remained intact (Table III). A similar pattern was also observed in a CORC® wires with 3 mm wide tapes after bending [2]. The I_c increase in Tapes 2 and 3 (Table III) was because the witness tapes measured at AMPeers were not identical to the tapes in Sample 1e. Although both groups of tapes were from the same batch, the witness tapes were shorter than the tapes in Sample 1e and they did not necessarily have the identical critical current.

To understand if the bending at different radii caused the degradation, we tested cable Sample 1f without bending. The results of cable Sample 1f were consistent with those of 1e. It was again the innermost and outermost tapes that degraded (Table IV). The degradation, however, was less severe in cable Sample 1f. This suggested that bending cable at different radii can cause further degradation, like in cable Sample 1e, but cannot solely explain the observed degradation.

The bending of Sample 1f with only the innermost tape did not further degrade the tape. The slight change in the critical current and n value after the bending was due to the measurement uncertainty in the current and the resulting uncertainty when fitting the measured $V(I)$ data using (1).

The results of cable Sample 1h shed more light on the degradation as observed in cable Samples 1e and 1f. The $V(I)$ comparison in Fig. 7 showed that the current at 20 μV degraded by 5% after the manual cabling process (Table V), much lower than those in cable Samples 1e and 1f. The current values in Table V characterized the critical current of the STAR® wire at different locations inside the termination. Although they are not the critical current of each individual tape in the STAR® wire, the comparison of the $V(I)$ curves suggested that the cabling process can have a minor impact on the critical current of the REBCO tapes.

We suspect that the large degradation in the innermost and outermost tapes in the wires used for the cable Samples 1e and 1f could have already occurred before the cabling process, possibly because of differences in architecture or fabrication process used for these wires. This can be verified, as a next step, by comparing the critical-current profile of each tape before and after being made into a STAR® wire [13], [14]. Equally important is to understand why the middle two tapes were robust through the entire fabrication process of both STAR® wires and 6-around-1 cables. The understanding can help manufacture STAR® wires with minimum degradation in REBCO tapes.

The $V(I)$ comparison in Fig. 7 was a better evaluation on the impact of cabling process than the comparison reported in [11]. Cable Sample 1h allowed a direct comparison between the $V(I)$ data thanks to the identical voltage-tap locations before and after the cabling process. The comparison reported in [11] is indirect, and therefore less accurate, because AMPeers and LBNL placed the voltage taps at different locations.

The improvement from the previously reported 20% degradation [11] was due to an improved comparison method, not

TABLE V
CABLE SAMPLE 1H. THE CURRENT DEFINED AT 20 μV, n VALUE AND RESISTIVE SLOPE DERIVED FROM EACH VOLTAGE SIGNAL, BEFORE AND AFTER THE MANUAL CABLING PROCESS. 77 K, SELF-FIELD.

Location	I before (A)	I after (A)	n before (-)	n after (-)	R before (nΩ)	R after (nΩ)	ΔI (-)	Δn (-)	ΔR (-)
V_4	225	213	4.1	4.4	43	41	-6%	6%	-5%
V_3	183	175	3.9	3.7	104	102	-4%	-4%	-2%
V_2	154	146	3.9	4.2	227	225	-5%	9%	-1%
V_1'	131	126	3.4	4.5	169	170	-4%	31%	1%
V_1	231	222	3.7	4.8	33	38	-4%	29%	16%

necessarily the cabling process. The 5% degradation is still high because we expect no degradation in the STAR® wire when we bend it to a 6-around-1 cable template. Assuming the STAR® wire was bent to a helical shape, the local bending radius was 56 mm along the longitudinal axis of the STAR® wire. The self-field effect on the STAR® wire, after cabling, cannot account for the 5% degradation either.

Another possible reason for the improved current retention can be fewer tapes in the STAR® wire. The previous cable samples used STAR® wires each having a larger diameter core and nine tapes [11]. The friction between the tapes can be higher and hence higher degradation during the cabling process compared to the 4-tape STAR® wires used here.

As a next step, we plan to make a 1.5 m long 6-around-1 cable using the cabling machine and six 1.3 mm diameter STAR® wires to further verify the current retention.

VI. CONCLUSIONS

We made and tested three 6-around-1 cable samples, each using a single STAR® wire containing four REBCO tapes. To understand the early voltage rise and degradation in the cable critical current, we quantified the current-carrying capability of each REBCO tape in the STAR® wire by successively measuring the $V(I)$ behavior of the cable sample after electrically eliminating one tape at a time from the STAR® wire. The two cable samples that used STAR® wires made with a 0.7-mm-diameter Nb-Ti former and 1.5, 1.8 and 2.3-mm-wide tapes consistently showed a strong degradation of the current-carrying capability, at least 30% – 60%, in the innermost and outermost tapes, although the middle two tapes remained intact even after one cable was bent to a 20 mm radius. We measured the $V(I)$ behavior of the STAR® wire, before and after being made into the third cable sample. This wire was made with 0.81-mm-diameter copper former with four 2-mm-wide tapes. We observed only a 5% decrease in the current of this STAR® wire after cabling. Therefore, the strong degradation in the innermost and outermost tapes in the first two STAR® wires may have occurred when manufacturing the wires. Our results showed how the current-carrying capability of the individual REBCO tapes in a STAR® wire changed in a 6-around-1 cable configuration. The results called for more detailed studies on the role of STAR® wire architecture and fabrication process to minimize the degradation of REBCO tapes.

ACKNOWLEDGMENT

We thank Eduard Galstyan who was with AMPeers for suggesting measuring the $V(I)$ behavior of outermost tapes by removing the tape from the STAR® wire.

One author, VS, has financial interest in AMPeers.

REFERENCES

[1] S. Prestemon, K. Amm, L. Cooley *et al.*, "The 2020 updated roadmaps for the US Magnet Development Program," http://arxiv.org/abs/2011.09539, Oct. 2020.

[2] J. D. Weiss, T. Mulder, H. J. ten Kate *et al.*, "Introduction of CORC® wires: highly flexible, round high-temperature superconducting wires for magnet and power transmission applications," *Superconductor Science and Technology*, vol. 30, no. 1, 014002, 2017, and references therein.

[3] D. C. van der Laan, J. D. Weiss, and D. M. McRae, "Status of CORC® cables and wires for use in high-field magnets and power systems a decade after their introduction," *Superconductor Science and Technology*, vol. 32, no. 3, 033001, February 2019, and references therein.

[4] W. Luo, S. Kar, X. Li *et al.*, "Superior critical current of symmetric tape round (STAR) REBCO wires in ultra-high background fields up to 31.2 T," *Superconductor Science and Technology*, vol. 31, no. 12, 12LT01, November 2018.

[5] A. Ben Yahia, S. Kar, G. Majkic *et al.*, "Modeling-driven optimization of mechanically robust REBCO tapes and wires," *IEEE Trans. Appl. Supercond.*, vol. 29, no. 5, Art. no. 8401605, August 2019.

[6] S. Kar, J. S. Sandra, W. Luo *et al.*, "Next-generation highly flexible round REBCO STAR wires with over 580 A mm^{-2} at 4.2 K, 20 T for future compact magnets," *Superconductor Science and Technology*, vol. 32, no. 10, 10LT01, August 2019.

[7] E. Galstyan, J. Kadiyala, M. Paidpilli *et al.*, "High critical current STAR® wires with REBCO tapes by advanced MOCVD," *Superconductor Science and Technology*, vol. 36, no. 5, 055007, Mar. 2023.

[8] X. Wang, D. Abraimov, D. Arbelaez *et al.*, "Development and performance of a 2.9 Tesla dipole magnet using high-temperature superconducting CORC® wires," *Superconductor Science and Technology*, vol. 34, no. 1, 015012, Dec. 2020.

[9] X. Wang, T. J. Bogdanof, P. Ferracin *et al.*, "An initial magnet experiment using high-temperature superconducting STAR® wires," *Superconductor Science and Technology*, vol. 35, no. 12, 125011, Nov. 2022.

[10] V. V. Kashikhin, S. Cohan, V. Lombardo *et al.*, "Accelerator magnet development based on COMB technology with STAR wires," *IOP conference series. Materials science and engineering*, vol. 1301, no. 1, 012153, May 2024.

[11] N. Castaneda, P. Ferracin, C. Funkhouser *et al.*, "A 6-around-1 cable using high-temperature superconducting STAR® wires for magnet applications," *Superconductor science & technology*, vol. 37, no. 3, 035009, Mar. 2024.

[12] P. Ferracin, G. Ambrosio, M. Anerella *et al.*, "Conceptual design of 20 T hybrid accelerator dipole magnets," *IEEE Trans. Appl. Supercond.*, vol. 33, no. 5, Art. no. 4002007, Aug. 2023.

[13] X. Hu, M. Small, K. Kim *et al.*, "Analyses of the plastic deformation of coated conductors deconstructed from ultra-high field test coils," *Superconductor Science and Technology*, vol. 33, no. 9, 095012, Aug. 2020.

[14] C.-M. Yang, Q.-F. Hong, C.-L. Chang *et al.*, "Effect of heating and bending on localized critical current in 2G HTS tapes with non-contact trapped field measurements," *Journal of materials research and technology*, vol. 32, pp. 2022–2029, Sep. 2024.